

N -to- Δ Electromagnetic-Transition Form Factors from Lattice QCD

C. Alexandrou,¹ Ph. de Forcrand,² H. Neff,³ J. W. Negele,⁴ W. Schroers,⁴ and A. Tsapalis¹

¹*Department of Physics, University of Cyprus, CY-1678 Nicosia, Cyprus*

²*ETH-Zürich, CH-8093 Zürich and Theory Division, CERN, CH-1211 Geneva 23, Switzerland*

³*Physics Department, Boston University, Massachusetts 02215, USA*

⁴*Center for Theoretical Physics, Laboratory for Nuclear Science and Department of Physics, Massachusetts Institute of Technology, Cambridge, Massachusetts 02139, USA*

(Received 19 September 2004; published 20 January 2005)

The magnetic dipole (M1), the electric quadrupole (E2), and the Coulomb quadrupole (C2) amplitudes for $\gamma N \rightarrow \Delta$ are calculated in quenched lattice QCD. Using a new method, which combines an optimal choice of interpolating fields for the Δ and an overconstrained analysis, we obtain statistically accurate results for the dipole form factor and for the ratios $R_{EM} = E2/M1$ and $R_{SM} = C2/M1$, up to momentum transfer squared 1.5 GeV^2 . We show for the first time, using lattice QCD, that both R_{EM} and R_{SM} are nonzero and negative, in qualitative agreement with experiment and indicating the presence of deformation in the N/Δ system.

DOI: 10.1103/PhysRevLett.94.021601

PACS numbers: 11.15.Ha, 12.38.Aw, 12.38.Gc, 14.70.Dj

Deformation is an important and well studied phenomenon in atomic and nuclear physics, and it is desirable to understand whether it also arises in low-lying hadrons and if so, why. For classical and quantum systems with spins larger than $1/2$, the one-body quadrupole operator provides a convenient characterization of deformation. Experimentally, however, in the excited spin $3/2$ Δ , which can have a nonzero quadrupole moment, it is not practical to measure it, and the spin $1/2$ nucleon, which is easily accessible to measurement, cannot have a spectroscopic quadrupole moment. Hence, the experiment of choice to reveal the presence of deformation in the low-lying baryons is measuring the N -to- Δ transition amplitude, and significant effort has been devoted to photoproduction and electroproduction experiments on the nucleon at LEGS [1], MAMI [2], Bates [3], and Jefferson Lab [4] in order to measure to high accuracy the ratios of the electric (E2) and Coulomb (C2) quadrupole amplitudes to the magnetic dipole (M1) amplitude. If both the nucleon and the Δ are spherical, then E2 and C2 are expected to be zero. Although M1 is indeed the dominant amplitude, there is mounting experimental evidence over a range of momentum transfers that E2 and C2 are nonzero [5]. Similarly in lattice QCD, for hadrons with spins larger than $1/2$, the deformation is determined by measuring their quadrupole moment knowing the hadron wave function, which can be obtained via density correlators [6,7]. Using these techniques, it was shown that the rho has a nonspherical spatial distribution with a nonzero quadrupole moment and that the Δ acquires a small deformation as the quark mass decreases [6]. However, direct contact with experiment is established by calculating the N -to- Δ transition form factors.

In this work we calculate these form factors as a function of the momentum transfer in lattice QCD in the quenched approximation on a lattice of size $32^3 \times 64$ at $\beta = 6.0$. We obtain, for the first time, accurate results for the E2 and C2

moments for momentum transfer squared, $-q^2$, up to about 1.5 GeV^2 . Our results are sufficiently accurate to exclude a zero value. The two novel aspects that are crucial for obtaining this accuracy are the following: (i) an optimal combination of three-point functions, which allows momentum transfers in a spatially symmetric manner obtained by an appropriate choice of the interpolating field for the Δ , and (ii) an overconstrained analysis using all lattice momentum vectors contributing to a given q^2 value in the extraction of the three transition form factors [8].

In lattice QCD, transitions with one-photon exchange, such as the N -to- Δ transition, require the evaluation of three-point functions, which involve the computation of a sequential propagator. The fixed current approach, used in previous lattice calculations [9,10], requires the current to have a fixed direction and to carry a fixed momentum. The initial and final states, on the other hand, can vary without requiring further inversions, which are the time-consuming part of the evaluation of three-point functions. In this work we use the fixed sink method in which the initial state, created at time zero, has the nucleon quantum numbers, and the final state, annihilated at a later fixed time t_2 , has the Δ quantum numbers. The current can couple to a quark line at any time slice t_1 carrying any possible value of the lattice momentum [7]. With the improvements implemented in this work, this method becomes clearly superior to the fixed current approach allowing accurate evaluation of the form factors.

The matrix element for the $\gamma N \rightarrow \Delta$ transition with on-shell nucleon and Δ states and real or virtual photons has the form [11]

$$\langle \Delta(p', s') | j_\mu | N(p, s) \rangle = i \sqrt{\frac{2}{3}} \left(\frac{m_\Delta m_N}{E_\Delta(\mathbf{p}') E_N(\mathbf{p})} \right)^{1/2} \bar{u}_\sigma(p', s') \times \mathcal{O}^{\sigma\mu} u(p, s), \quad (1)$$

where $p(s)$ and $p'(s')$ denote initial and final momenta (spins) and $u_\sigma(p', s')$ is a spin vector in the Rarita-Schwinger formalism. The operator $\mathcal{O}^{\sigma\mu}$ can be decomposed in terms of the Sachs form factors as

$$\mathcal{O}^{\sigma\mu} = \mathcal{G}_{M1}(q^2)K_{M1}^{\sigma\mu} + \mathcal{G}_{E2}(q^2)K_{E2}^{\sigma\mu} + \mathcal{G}_{C2}(q^2)K_{C2}^{\sigma\mu}, \quad (2)$$

where the magnetic dipole, \mathcal{G}_{M1} , the electric quadrupole, \mathcal{G}_{E2} , and the Coulomb quadrupole, \mathcal{G}_{C2} , form factors depend on the momentum transfer $q^2 = (p' - p)^2$. The kinematical functions $K^{\sigma\mu}$ in Euclidean space are given in Ref. [10]. Using the relations given in Refs. [11,12] the

ratios R_{EM} and R_{SM} in the rest frame of the Δ are obtained from the Sachs form factors via

$$R_{EM} = -\frac{\mathcal{G}_{E2}(q^2)}{\mathcal{G}_{M1}(q^2)}, \quad R_{SM} = -\frac{|\mathbf{q}|}{2m_\Delta} \frac{\mathcal{G}_{C2}(q^2)}{\mathcal{G}_{M1}(q^2)}. \quad (3)$$

The ratio R_{EM} is also known as EMR and R_{SM} as CMR.

To extract the N -to- Δ matrix element from lattice measurements we calculate, besides the three-point function $G_\sigma^{\Delta j^\mu N}(t_2, t_1; \mathbf{p}', \mathbf{p}; \Gamma)$, the nucleon and Δ two-point functions, G^{NN} and $G_{ij}^{\Delta\Delta}$, and look for a plateau in the large Euclidean time behavior of the ratio

$$R_\sigma(t_2, t_1; \mathbf{p}', \mathbf{p}; \Gamma; \mu) = \frac{\langle G_\sigma^{\Delta j^\mu N}(t_2, t_1; \mathbf{p}', \mathbf{p}; \Gamma) \rangle}{\langle G_{ii}^{\Delta\Delta}(t_2, \mathbf{p}'; \Gamma_4) \rangle} \left[\frac{\langle G^{NN}(t_2 - t_1, \mathbf{p}; \Gamma_4) \rangle \langle G_{ii}^{\Delta\Delta}(t_1, \mathbf{p}'; \Gamma_4) \rangle \langle G_{ii}^{\Delta\Delta}(t_2, \mathbf{p}'; \Gamma_4) \rangle}{\langle G_{ii}^{\Delta\Delta}(t_2 - t_1, \mathbf{p}'; \Gamma_4) \rangle \langle G^{NN}(t_1, \mathbf{p}; \Gamma_4) \rangle \langle G^{NN}(t_2, \mathbf{p}; \Gamma_4) \rangle} \right]^{1/2} \\ \xrightarrow{t_2 - t_1 \gg 1, t_1 \gg 1} \Pi_\sigma(\mathbf{p}', \mathbf{p}; \Gamma; \mu). \quad (4)$$

We use the lattice conserved electromagnetic current, $j^\mu(x)$, symmetrized on site x and projection matrices for the Dirac indices

$$\Gamma_i = \frac{1}{2} \begin{pmatrix} \sigma_i & 0 \\ 0 & 0 \end{pmatrix}, \quad \Gamma_4 = \frac{1}{2} \begin{pmatrix} I & 0 \\ 0 & 0 \end{pmatrix}. \quad (5)$$

Throughout this work we use kinematics where the Δ is produced at rest and therefore $\mathbf{q} = \mathbf{p}' - \mathbf{p} = -\mathbf{p}$. We fix $t_2 = 12$ in lattice units and search for a plateau of $R_\sigma(t_2, t_1; \mathbf{p}', \mathbf{p}; \Gamma; \mu)$ as a function of t_1 . $Q^2 = -q^2$ denotes the Euclidean momentum transfer squared.

We can extract the three Sachs form factors from the ratio of Eq. (4) by choosing appropriate combinations of σ indices and Γ matrices. However, there are several choices of σ indices and Γ matrices that can be used, each requiring an inversion, and therefore we must determine the most suitable combination. For example, the dipole form factor can be extracted from

$$\Pi_\sigma(\mathbf{q}; \Gamma_4; \mu) = iA e^{\sigma 4 \mu j} p^j \mathcal{G}_{M1}(Q^2), \quad (6)$$

where A is a kinematical coefficient. This means that there are six statistically independent matrix elements to extract \mathcal{G}_{M1} , each requiring the evaluation of a sequential propagator. However, due to the epsilon factor, a choice of one of the six combinations means that only momentum transfers in one direction contribute. Instead, if we take the symmetric combination,

$$S_1(\mathbf{q}; \mu) = \sum_{\sigma=1}^3 \Pi_\sigma(\mathbf{q}; \Gamma_4; \mu), \quad (7)$$

lattice momentum vectors in all directions contribute. This combination, referred to as sink type S_1 , is built into the Δ interpolating field and requires only one inversion.

Another choice of three-point functions is to use the projection matrices Γ_k instead of Γ_4 . The relations are more involved in this case and will be discussed in detail elsewhere. However, as in the example given in Eq. (6),

instead of choosing one of six we can consider a linear combination that involves, in a symmetric manner all spatial directions allowing, for a given Q^2 , the maximum number of momentum vectors to contribute. We take

$$S_2(\mathbf{q}; \mu) = \sum_{\sigma \neq k=1}^3 \Pi_\sigma(\mathbf{q}; \Gamma_k; \mu), \quad (8)$$

which we refer to as sink S_2 . When the current is in the spatial direction both \mathcal{G}_{E2} and \mathcal{G}_{C2} can be extracted from S_2 with one inversion. In addition, when the current is in the time direction, S_2 provides a statistically independent way for evaluating \mathcal{G}_{C2} , with no extra cost. Another combination to extract \mathcal{G}_{E2} and \mathcal{G}_{C2} is $S_3(\mathbf{q}; \mu) = \Pi_3(\mathbf{q}; \Gamma_3; \mu) - [\Pi_1(\mathbf{q}; \Gamma_1; \mu) + \Pi_2(\mathbf{q}; \Gamma_2; \mu)]/2$, which produces results of comparable quality to those obtained with S_2 [13]. In the case of E2, sink type S_3 has the disadvantage of vanishing at the lowest value of Q^2 , whereas S_2 contributes at all values of Q^2 . For C2, on the other hand, S_2 gives zero at the lowest Q^2 , whereas source type S_3 gives a nonvanishing result.

The second important ingredient in the extraction of the form factors is to take into account in our analysis all the lattice momentum vectors that contribute to a given Q^2 . This is done by solving the overcomplete set of equations

$$P(\mathbf{q}; \mu) = D(\mathbf{q}; \mu)F(Q^2), \quad (9)$$

where $P(\mathbf{q}; \mu)$ are the lattice measurements of the ratio given in Eq. (4) having statistical errors w_k and using the different sink types,

$$F = \begin{pmatrix} \mathcal{G}_{M1} \\ \mathcal{G}_{E2} \\ \mathcal{G}_{C2} \end{pmatrix}$$

and, with N being the number of current directions and momentum vectors contributing to a given Q^2 , D is an $N \times 3$ matrix which depends on kinematical factors. We extract the form factors by minimizing

$$\chi^2 = \sum_{k=1}^N \left(\frac{\sum_{j=1}^3 D_{kj} F_j - P_k}{w_k} \right)^2, \quad (10)$$

using the singular value decomposition of D .

All the results for the form factors are obtained using 200 configurations and three values of the hopping parameter κ . The values of κ chosen are 0.1554, 0.1558, and 0.1562 and give ratio of pion to rho mass $m_\pi/m_\rho = 0.64, 0.59, \text{ and } 0.50$, respectively. We use the nucleon mass at the chiral limit to set the lattice spacing a obtaining $a^{-1} = 2.04(2)$ GeV ($a = 0.098$ fm). Using the optimized sink S_1 we show in Fig. 1 at the three quark masses our results for the Ash form factor \mathcal{G}_m^* defined by [18]

$$\mathcal{G}_m^*(Q^2) = \frac{1}{\sqrt{1 + \frac{Q^2}{(m_N + m_\Delta)^2}}} \mathcal{G}_{M1}(Q^2). \quad (11)$$

To obtain the results at the chiral limit, shown in the same figure, we perform a linear extrapolation in m_π^2 . Although we expect chiral logs that appear at next-to-leading order in chiral perturbation theory to be suppressed for the momentum transfers studied in this work, our linear extrapolation introduces a systematic uncertainty. This uncertainty cannot be assessed, since the known chiral perturbation theory results [12,19] are valid at very low masses and momentum transfers. In the same figure we also show the experimental values [3,4,14–17]. We perform fits to both the lattice data at the chiral limit and the experimental data using the phenomenological parametrization

$$\mathcal{G}_a(Q^2) = \mathcal{G}_a(0) R_a(Q^2) G_E^p(Q^2), \quad (12)$$

where $R_a(Q^2)$ for $a = M1, E2, \text{ and } C2$ measures the deviations from the proton electric form factor $G_E^p(Q^2) = 1/(1 + Q^2/0.71)^2$. Usually experimental data are fitted by taking $R_{M1}(Q^2) = R_{E2}(Q^2) = R_{C2}(Q^2) = (1 + \alpha Q^2) \times$

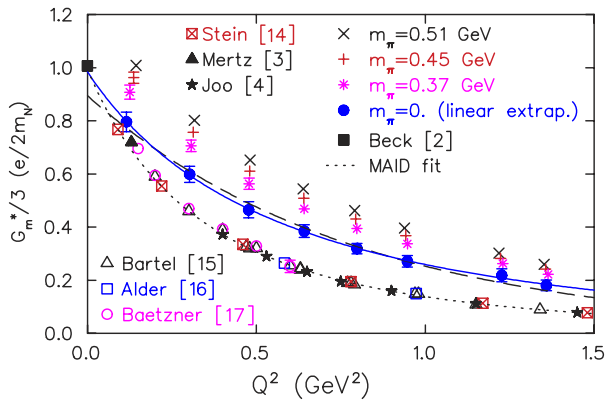


FIG. 1 (color online). \mathcal{G}_m^* as a function of Q^2 . Lattice results at $\kappa = 0.1554$ are shown by the crosses, at $\kappa = 0.1558$ by the open triangles, and at $\kappa = 0.1562$ by the asterisks. The filled circles show linear extrapolations. The solid and dotted lines are fits using the ansatz of Eq. (12). The dashed line is a fit to the lattice data using the ansatz $a \exp(-bQ^2)$.

$\exp(-\gamma Q^2)$ [20,21], which provides a very good fit to experiment and has been used in Fig. 1. Although the lattice data at the chiral limit lie higher than the experimental data, they can be fitted to the same ansatz yielding at $Q^2 = 0$ a value consistent with experiment [2]. The lattice data are also well described by the simple exponential ansatz $a \exp(-bQ^2)$, which, however, at $Q^2 = 0$ gives a value lower than experiment.

Using the optimized sink S_2 we extract the quadrupole form factors, \mathcal{G}_{E2} and \mathcal{G}_{C2} , at three values of the quark mass, as shown in Figs. 2 and 3 with the exception of \mathcal{G}_{C2} at the lowest Q^2 value extracted using S_3 . In the same figures we also show the values obtained in the chiral limit by performing a linear extrapolation in m_π^2 . As expected, both EMR and CMR become more negative as we approach the chiral limit. Since the asymmetry persists to sufficiently high quark masses and we are aware of no lattice artifacts that would account for it, it is likely that some other mechanism besides the pion field is responsible for it. Our results for EMR and CMR at the chiral limit are compared to recent measurements [1–4,22] in Figs. 2 and 3, respectively. The quenched results for EMR are accurate enough to exclude a zero value at low Q^2 . With our current statistics they are in agreement with the experimental measurements. Whether the apparent discrepancy for CMR at low Q^2 is a significant deficiency of quenched QCD or a problem with the two data points remains to be resolved by new measurements that are currently being

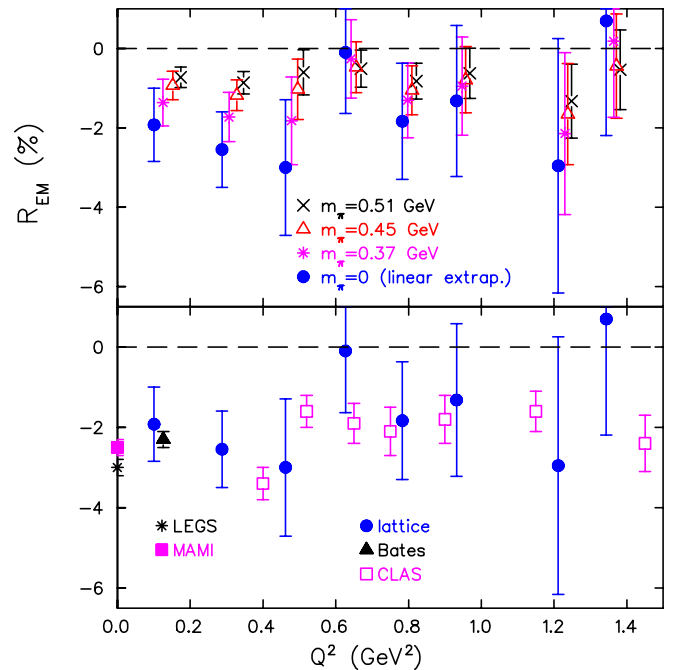


FIG. 2 (color online). R_{EM} as a function of Q^2 . The upper graph shows our lattice results in the same notation as Fig. 1. The lower graph shows recent experimental results: [1] (asterisks), [2] (filled squares), [3] (filled triangles), and [4] (open squares).

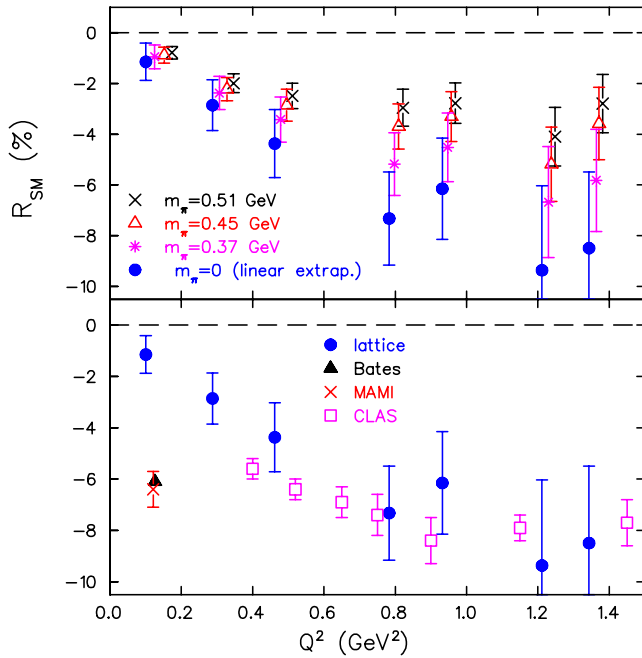


FIG. 3 (color online). R_{SM} as a function of Q^2 . The notation is the same as in Fig. 2.

analyzed. As Q^2 increases, however, the quenched results agree qualitatively with measurements.

In summary, two novel methods are applied to the evaluation of the N -to- Δ transition form factors: The first improvement comes from employing an optimized sink for the Δ allowing a maximum number of lattice matrix elements to contribute, and the second from utilizing this enlarged set of data in an overconstrained analysis. Given that there are ambiguities in the extraction of the quadrupole amplitudes from experimentally measured response functions arising from using models, accurate lattice data are extremely valuable: excluding a zero quadrupole strength in lattice QCD corroborates experimental observations for a nonzero R_{EM} and R_{SM} . In addition, the sign of R_{EM} and R_{SM} is unambiguously determined and in agreement with experiment. This is particularly important for CMR where at low Q^2 there are very few accurate experimental measurements. If confirmed, the agreement of EMR with experiment at low Q^2 while CMR disagrees with experiment raises interesting questions regarding the pion cloud contributions to these ratios due to the absence of the sea quarks. Having, for the first time, demonstrated that we can reliably extract CMR in quenched lattice QCD opens the way for a precise investigation of sea quark contributions to both EMR and CMR, which can lead to

an understanding of the physical mechanism responsible for nonzero quadrupole strength in the N -to- Δ transition.

A. T. is supported by the Levendis Foundation, and W. S. is partially supported by the Alexander von Humboldt Foundation. This research used resources of the National Energy Research Scientific Computing Center, which is supported by the Office of Science of the U.S. Department of Energy under Contract No. DE-AC03-76SF00098. This work is supported in part by the U.S. Department of Energy (DOE) under Cooperative Research Agreements No. DF-FC02-94ER40818 and No. DE-FC02-01ER41180.

-
- [1] G. Blanpied *et al.*, Phys. Rev. Lett. **79**, 4337 (1997).
 - [2] R. Beck *et al.*, Phys. Rev. C **61**, 035204 (2000).
 - [3] C. Mertz *et al.*, Phys. Rev. Lett. **86**, 2963 (2001); N. Spaveris *et al.*, this issue, Phys. Rev. Lett. **94**, 022003 (2005).
 - [4] K. Joo *et al.*, Phys. Rev. Lett. **88**, 122001 (2002).
 - [5] C. N. Papanicolas, Eur. Phys. J. A **18**, 141 (2003); A. M. Bernstein, Eur. Phys. J. A **17**, 349 (2003).
 - [6] C. Alexandrou, Ph. de Forcrand, and A. Tsapalis, Phys. Rev. D **66**, 094503 (2002); Phys. Rev. D **68**, 074504 (2003); Nucl. Phys. (Proc. Suppl.) **119**, 422 (2003); Nucl. Phys. **A721**, 907 (2003); Nucl. Phys. (Proc. Suppl.) **129**, 221 (2004).
 - [7] C. Alexandrou, Nucl. Phys. (Proc. Suppl.) **128**, 1 (2004).
 - [8] LHPC and SESAM Collaborations, Ph. Hagler *et al.*, Phys. Rev. D **68**, 034505 (2003).
 - [9] D.B. Leinweber, T. Draper, and R.M. Woloshyn, Phys. Rev. D **48**, 2230 (1993).
 - [10] C. Alexandrou *et al.*, Phys. Rev. D **69**, 114506 (2004); Nucl. Phys. (Proc. Suppl.) **129**, 302 (2004).
 - [11] H.F. Jones and M.C. Scadron, Ann. Phys. (N.Y.) **81**, 1 (1973).
 - [12] G.C. Gellas, T.R. Hemmert, C.N. Ktorides, and G.I. Poulis, Phys. Rev. D **60**, 054022 (1999).
 - [13] C. Alexandrou *et al.*, hep-lat/0408017.
 - [14] S. Stein *et al.*, Phys. Rev. D **12**, 1884 (1975).
 - [15] W. Bartel *et al.*, Phys. Lett. **28B**, 148 (1968).
 - [16] J.C. Alder *et al.*, Nucl. Phys. **B46**, 573 (1972).
 - [17] K. Bätzner *et al.*, Phys. Lett. **39B**, 575 (1972).
 - [18] W.W. Ash, K. Berkelman, C.A. Lichtenstein, A. Ramanauskas, and R.H. Siemann, Phys. Lett. **24B**, 165 (1967).
 - [19] D. Arndt and B.C. Tiburzi, Phys. Rev. D **69**, 014501 (2004).
 - [20] D. Drechsel, O. Hanstein, S.S. Kamalov, and L. Tiator, Nucl. Phys. **A645**, 145 (1999); L. Tiator *et al.*, Nucl. Phys. **A689**, 205 (2001).
 - [21] T. Sato and T.-S.H. Lee, Phys. Rev. C **63**, 055201 (2001).
 - [22] Th. Pospischil *et al.*, Phys. Rev. Lett. **86**, 2959 (2001).